Isaac Fitts-Sprague
413 Honors Project
Professor James Rinderle

1. Project Background

At my house, we have a pivoting gate that can be put across our driveway so that our yard is completely fenced in. This allows us to let our dog roam free without having to worry about her running away.

While this gate is extremely useful, it can be an enormous hassle. If you want to let the dog out and the gate is not already shut, you need to leave the backyard and manually move the gate. In bad weather and cold conditions this can be frustrating and difficult. If you are backing your car out of the driveway, you need to open the gate before you get in the car, then back out of the driveway and get out of your car again to close the gate before you drive away. This is done multiple times every day.

A device is needed to safely and reliably close and open the gate via a remote control.

General Requirements:

- The system should be able to go from a fully closed position to a fully open position, and vice versa, in 20 seconds or less.
- The system should be as low maintenance and as durable as possible.
- The system should not be exuberantly expensive.
- The system should take up as little space in the driveway as possible and not be a tremendous eye sore.
- The system should not have any dangerous exposed components or areas where the dog could damage it.

2. Design Configurations

a. Gate Overview

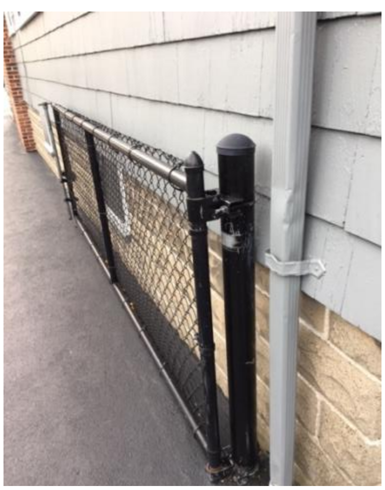

Figure 1. Picture of the gate fully open.

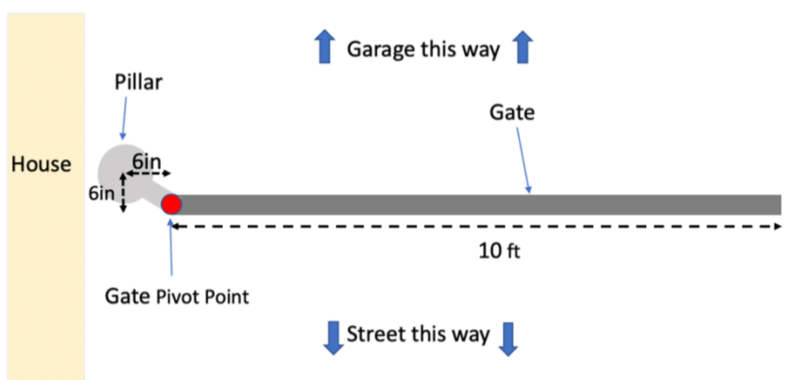

Figure 2. Birds eye view diagram of the gate in the closed position.

Figures 1 and 2, shown above, specify the dimensions of the gate. When the gate is open, there is less than six inches of clearance between the house and the gate. The pillar the gate rotates around is also only 12 inches away from the house. The driveway is already narrow, so any prospective device must not extend far into the driveway.

b. Analysis/Design Strategy

I chose to design three different mechanical assemblies that could be attached to the existing gate to allow it to be automatically opened and closed. The three assemblies are diverse as to demonstrate the number of design options that could be implemented to accomplish this objective.

Once the general concept behind each assembly was developed, I mathematically modeled them to find relationships between required actuating force, torque, motor placement, device placement, and other sizing parameters. In almost every case increasing system dimensions was advantageous, but this was restricted to a point based on the amount of available driveway space.

As the designs are quite different, a strategy was developed to rank qualities and parameters of each assembly such as cost, driveway obstruction, weather sensitivity, etc. These rankings were used to quantify each assemblies' strengths and weaknesses to determine which would work best.

In all of the following analysis it is assumed that the gate has no mass and requires a torque of 80 lbf*ft to rotate.

c. Pulley System

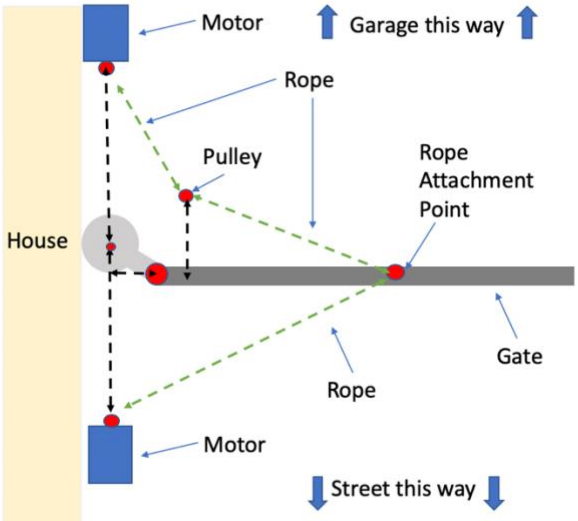

Figure 3. Diagram of the pulley system in the closed position with all motors and ropes shown. Gate opens towards the street.

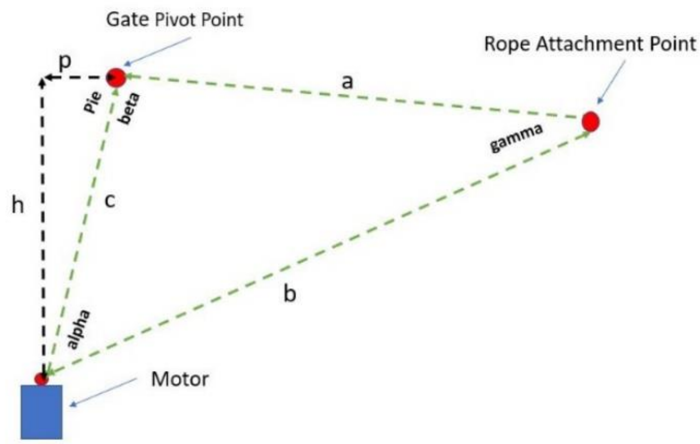

Figure 4. Opening pulley system diagram used for analyzing and optimizing the assembly. Gate represented as line a, nearly fully closed.

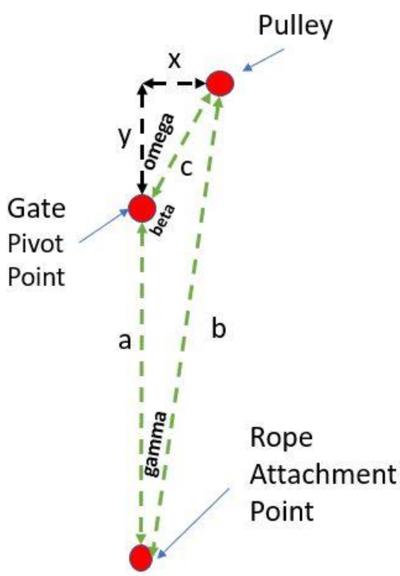

Figure 5. Closing pulley system diagram used for analyzing and optimizing the assembly. Gate represented as line a, fully open.

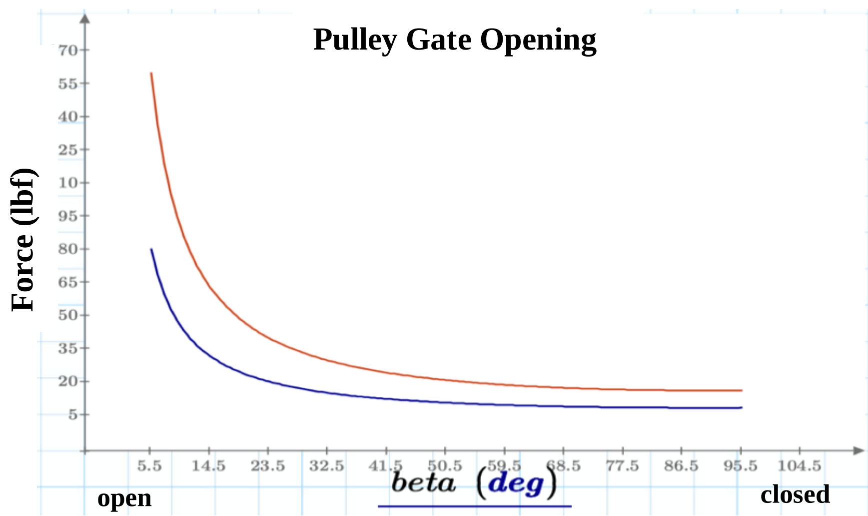

Figure 6. Graph of the required force to open the gate using the pulley. The red line indicates a system where the length of h (shown in figure 4) is 10 ft and the blue line indicates a system where the length of h is 5ft.

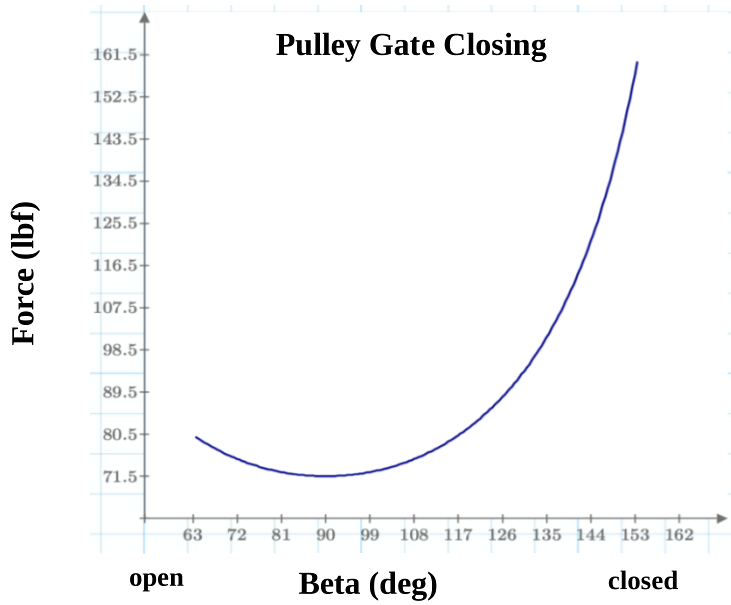

Figure 7. Graph of the required force to close the gate using the pulley.

The pulley system design is shown in figures 3, 4 and 5. This design was analyzed and the force requirements for opening and closing the gate using this system can be seen in figure 6 and 7 respectively. From these results, it can be noted that making the length of both h and p (shown in figure 4) as large as possible reduces the required rope pulling force. However, for practicality purposes, h was limited to 10 feet and p was limited to 6 inches so as not to obstruct the driveway.

The relationship between the required force to open the gate and the gate position, shown in figure 6, shows that the required rope force significantly increases as the gate gets closer to being fully open.

For the closing system, shown in figure 5, X was limited at 6 inches and Y was limited to 1 foot so they driveway would not be obstructed. The analysis showed that increasing X and Y as much as possible reduced the required rope pulling force. A plot showing the relationship between closing force and gate position is shown in figure 7. This figure shows that a significant amount of force is required to close the gate even when all of the gates geometric parameters are set to their maximum limit.

This system, unlike the other two that will be discussed, requires two individual motors to be placed on either side of the gate. Additionally, when the pulley system is in operation, both motors will have to work together in sync to ensure that the motor not pulling the gate is producing enough slack so that no extra pulling resistance is added. This requirement adds complexity to the overall assembly and provides another area where the design could malfunction. The requirement of two motors and the associated pulley, gear systems, and electronics also increases the cost.

d. Belt System

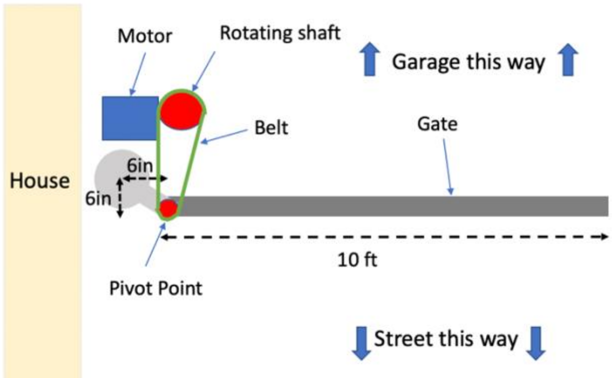

Figure 8. Blet system with the gate in the closed position.

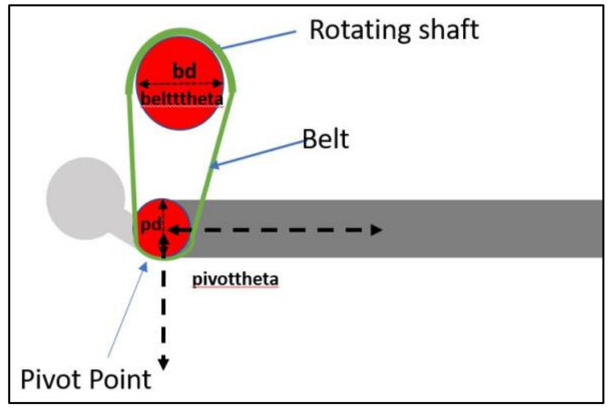

Figure 9. Belt system diagram.

The belt assembly is shown above in figure 8, and design specifications are shown in figure 9. This assembly involves attaching a belt/band to the pivot post of the gate and using a motor and gear system to rotate the gate open and closed. This design is extremely simple compared to the other two and requires the least amount of parts.

One disadvantage of the belt opener is the space it would occupy in the driveway. Due to the shape of this system it would likely be less intrusive than the pulley system, but the motor, gear box, and belt could be at risk of being bumped into or damaged by passing cars.

This belt assembly could also be negatively affected in bad weather. In snowy, icy, or wet conditions the friction between the belt and the pivot rod could be reduced. This could possibly stop the assembly from working all together or increase the amount of time the gate would take to move from one position to another.

e. Lead Screw

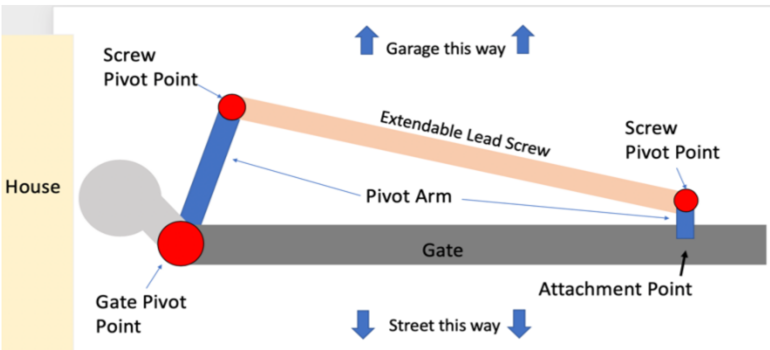

Figure 10. Lead screw system overview.

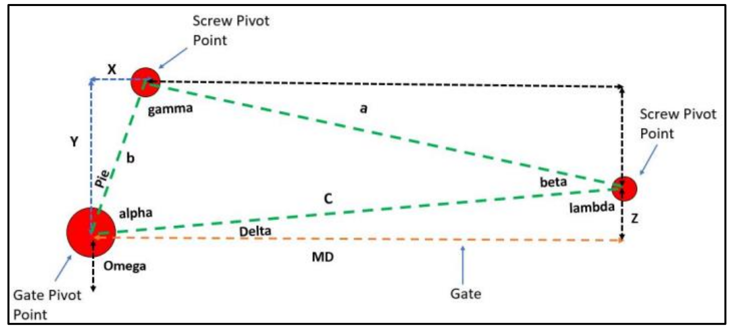

Figure 11. Lead screw system diagram used to calculate forces and optimize the system.

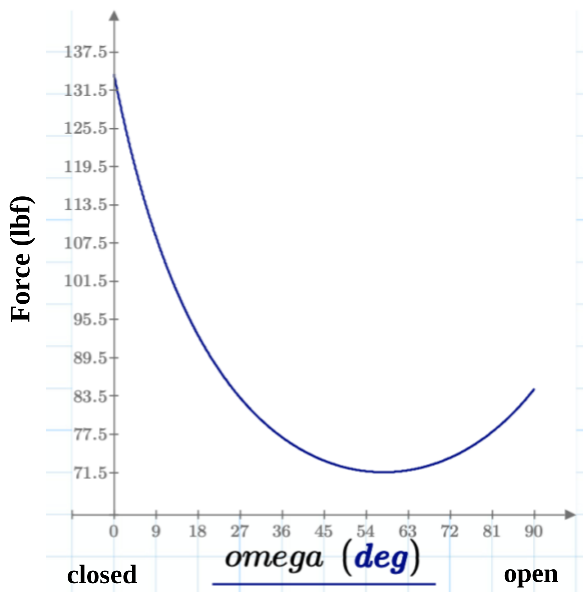

Figure 12. Required force to open and close the gate using the lead screw.

The lead screw system design overview is shown in figures 10 and 11. The lead screw consists of a fixed pivot arm mounted to the gate pivot point, which does not rotate or move, and another pivot arm that is attached to the gate which also does not move or rotate relative to the gate. This design works by having the lead screw slowly extend or retract, opening or closing the gate in the process. While both pivot arms are fixed, the lead screw can rotate where it is secured to the pivot points on both ends. Increasing the length of Z, X, and Y (shown in figure 11) all reduce the required screw force to move the gate. However, X and Z cannot be greater than 6 inches, and Y 12 inches, to avoid being an obstruction in the driveway. A plot of the actuation force vs the gate position for the optimized lead screw system geometry is shown in figure 12.

This lead screw design would be more complicated than the belt system, but still less complicated than the pulley system according to the number of parts required. Additionally, weather would not impact the performance of the lead screw system because the entire device could be made inside a weatherproof housing. This system would also require zero space on the ground and could be completely self-contained when hanging off the side of the gate.

3. Design Comparison and Selection

Each of the three designs proposed above could be implemented and made to work in the given scenario, however there are still clear advantages and disadvantages to some designs over others. To compare these designs, a list of important criteria was developed according to how the consumer (my family) would use the product. Each criterion was given a weight according to how important it is to the function of the system, shown below in table 1.

The most important criterion were determined to be: maintenance, reliability in bad weather, ease of installation, durability, and the hazard the design poses in the driveway. It's important to note that this is a subjective ranking system and should not be taken to be absolutely correct. Each person conducting this selection process could arrive at a different result. Acording to my analysis, the lead screw scored well above the others leading to its selection as the final design.

Major comparison highlights:

For the belt opener to work, their needs to be a significant amount of tension in the belt between the rotating shaft and the gate pivot shaft, shown in figure 9. Maintaining this tension in all weather, over long periods of time, and with lots of use is expected to be difficult. This factor reduced the score the belt opener received for reliability in bad weather, expected maintenance, and durability.

Additionally, for the belt opener to work, the existing gate would need to be significantly altered so that the gate pivot shaft could be attached to the belt. The gate pivot shaft holds the entire weight of the gate, so this would require either skilled modification of the existing shaft, or a custom shaft be created. Either way this would significantly add to the complexity of the installation and the cost of the system.

The pulley system scored significantly worse than all of the other designs. The pulley system requires more parts and would require an involved installation to secure both motors and ropes on the gate and on the driveway.

The pulley system is also expected to have extremely high maintenance requirements. This is because the ropes would be very intrusive in the driveway and could end up snagging on objects or dragging on the ground. The ropes would also be subject to intense weather, causing additional wear. In snow and icy conditions, it is also possible the snow and ice would collect on the rope and get pulled into the motor/pulley system when the system is in in operation, posing a threat to the entire device.

The lead screw has relatively few components, would require minimal installation or modification to the existing gate, and would not be exposed or influenced by the weather. Unlike the belt and pulley systems that would need to employ a rope or a flexible belt, the lead screw could be designed out of durable, non-flexible material, increasing its operational lifetime. Compared to the pulley system, the lead screw also has a low actuation force which does not fluctuate significantly as the gate changes position, unlike the pulley system.

Table 1. Design comparison chart with weighted criteria. In the ranking system 1 represents the worst possible score and 5 represents the best.

		Lead Screw		Pulley System		Belt Opener	
Selection Criteria	**Weight**	Rating (1-5)	Weighted Score	Rating (1-5)	Weighted Score	Rating (1-5)	Weighted Score
Low cost	10%	4	0.4	2	0.2	4	0.4
Reliability in bad weather	15%	5	0.75	3	0.45	3	0.45
Expected maintenance	20%	5	1	1	0.2	1	0.2
Ease of installation	15%	4	0.6	1	0.15	1	0.15
Appearance	5%	3	0.15	1	0.05	5	0.25
Durability	15%	5	0.75	2	0.3	3	0.45
Driveway Hazard	15%	2	0.3	2	0.3	3	0.45
Actuation Force	5%	5	0.25	1	0.05	2	0.1
	Total Score	4.2		1.7		2.45	
	Rank	1		3		2	

4. Lead Screw System Design

This system was designed with the screw first, then the motor was selected, then the required gear system was designed. The screw was chosen to be designed first because it's efficiency and torque requirements directly impact what motor is needed and what gear ratio is needed to accompany it.

a. Screw Design

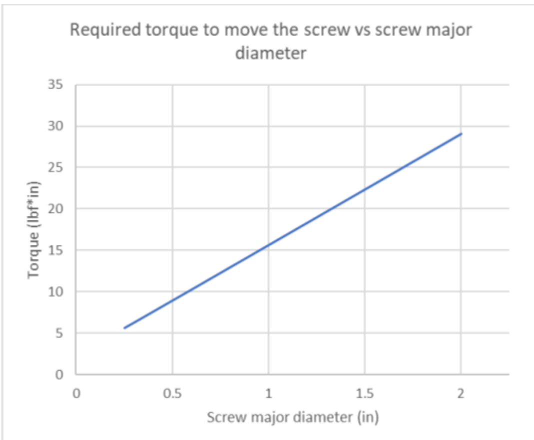

Figure 13. Required torque to rotate the lead screw vs screw major diameter calculated using the max force that would be required to move the gate.

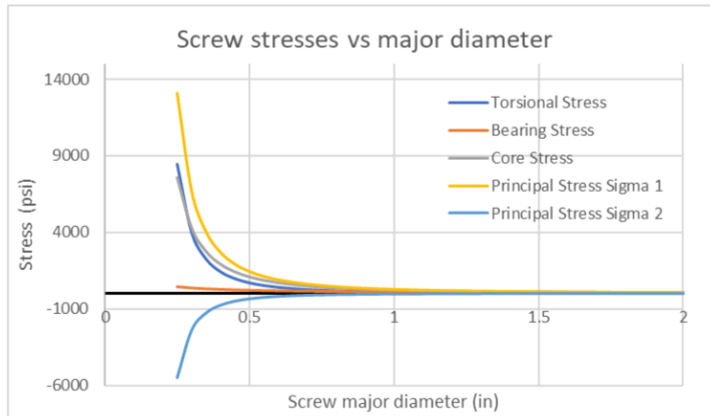

Figure 14. Screw stresses vs major diameter for screws with 10 threads per inch. Max torsional stress is ignored because the principal stresses are greater.

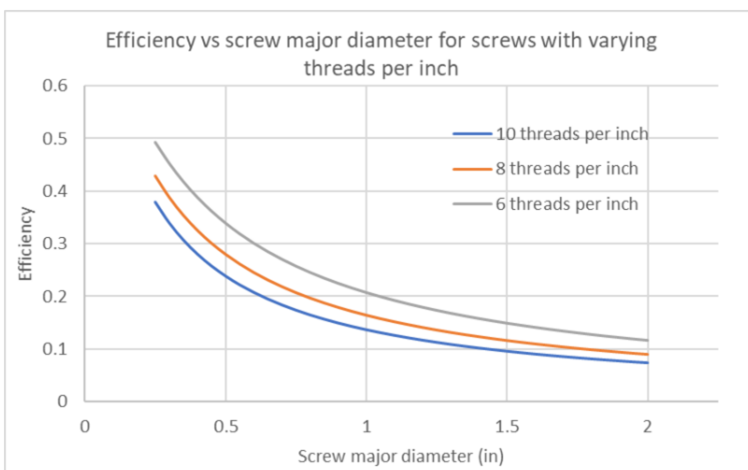

Figure 15. The efficiency of the screw vs the screw major diameter for screws with varying threads per inch. The greater the diameter of the screw, the less efficient it is.

A single lead screw was selected from table 10.3 in “Fundamentals of Machine Component Design: 5th addition”, titled “standard sizes of power screw threads”. The lead screw was assumed to have a single square thread, a coefficient of friction of 0.2, and a yield stress of 36 ksi. It was also assumed the screw would be mated to a 1-inch thick bolt which would be rotated by the motor to either extend or retract the screw, driving the gate.

Efficiency was of particular importance here because the motor used in the lead screw system is likely to be the most expensive component. By choosing the most efficient lead screw, it will lead to a lower power requirement from the motor, decreasing the size of the motor needed and therefore lowering the cost.

Under these assumptions, figures 13, 14, and 15 were generated to assess the efficiency, required actuating torque, and stresses the screw would experience for a variety of major screw diameters. These stresses were calculated according to the max tensile force the lead screw would experience of approximately 132 lbf, shown in figure 12. These plots show that decreasing the major screw diameter raises the efficiency and stresses experienced but lowers the required actuation torque.

Using this information, table 2 was generated to compare the screws with the smallest major diameter in table 10.3 of the textbook. The smallest screw, with a major diameter of 0.25 inches, was selected as it has the greatest efficiency, and lowest actuating torque of all the options, while experiencing stresses far below the materials yield strength. A plot of the required torque to rotate this lead screw vs the gate angle is shown in figure 16 below.

Table 2. Important design parameters for power screws listed in table 10.3 of the textbook “Fundamentals of Machine Component Design: 5th addition”.

Book Values		Calculated Parameters					
d (in)	Threads Per Inch	Efficiency	T screw (lbf *in)	Torsional Stress (psi)	Bearing Stress (psi)	Core Stress (psi)	Principal Sigma 1 (psi)
0.250	10	0.38	5.63	8489.68	426.54	7582.85	13089.25
0.313	10	0.33	6.45	3424.22	324.98	3778.31	5799.93
0.375	10	0.29	7.28	1783.12	262.48	2256.05	3237.99
0.375	8	0.34	7.86	2561.18	272.98	2729.83	4267.09
0.438	8	0.31	8.69	1449.63	227.49	1747.09	2566.03
0.500	6.5	0.32	10.18	1250.06	201.63	1423.89	2150.52
0.625	5.2	0.32	12.73	800.04	161.31	911.29	1376.34

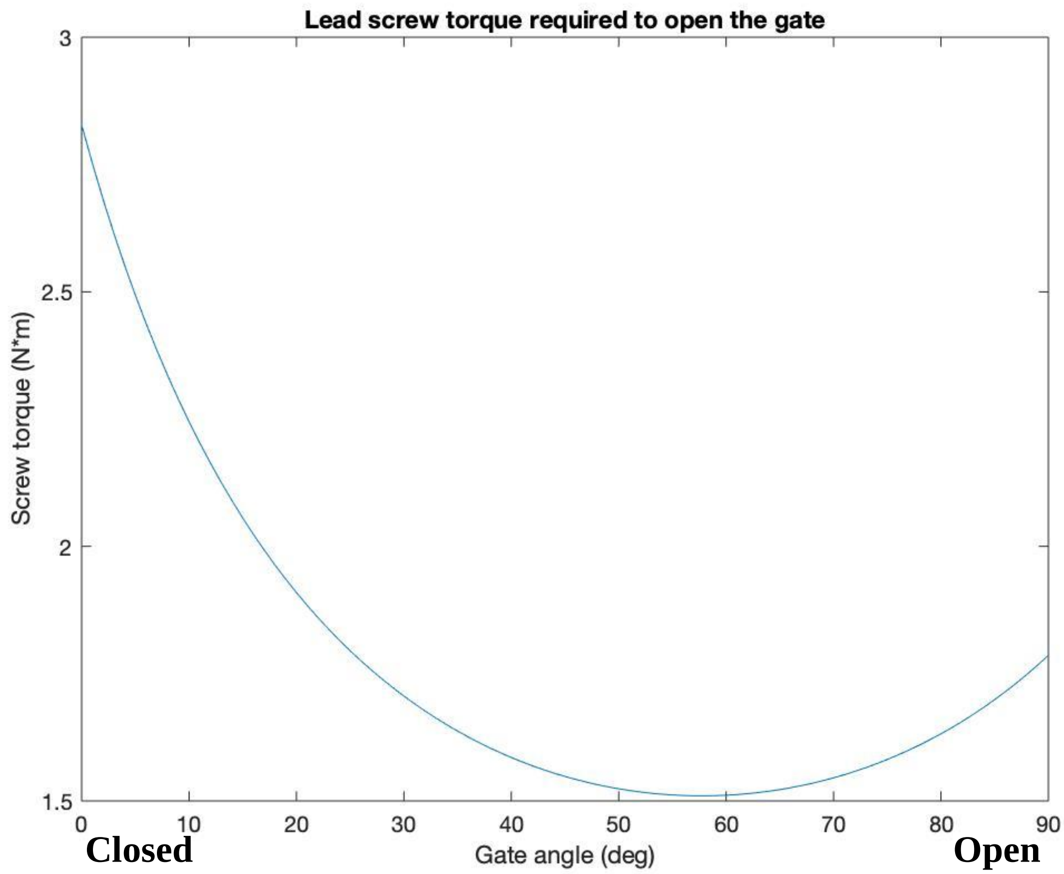

Figure 16. Plot of the required lead screw torque to open the gate.

b. Motor Selection

For the motor selection, it is assumed a 24V power supply from two car batteries wired in series would be used to power the gate opener.

When deciding which motor to select for this design, an important consideration was the amount of time the motor would be continuously operating. It was decided that the motor should be able to operate about 10 minutes at a time (to simulate the motor getting stuck) before the motor overheats. Based on this design parameter, a 10-minute duty curve was developed for each motor by modifying the continuous duty curve for each motor. This process is described below.

In the continuous duty equation, shown below in equation 1, TPR is essentially the reciprocal of the overall heat transfer coefficient, hA, in a heat transfer equation. This allows one to say that $\frac{\Delta T}{TPR}$ is the steady rate of heat transfer for the motor during continuous duty. A max ΔT of 75C can be tolerated, so the max continuous internal power dissipation of a motor is $\frac{75C}{TPR}$. However, since in my case the motor will not be operating continuously and will only be operating for a maximum of 10 minutes at a time, the average internal motor power dissipation can be higher.

Equation 1. Equation for the continuous duty torque speed curve of a motor.

$$T_L = \sqrt{\left(\frac{\Delta T}{TPR} - T_F * \omega - F_i * \omega^w\right) * \frac{{K_T}^2}{R_M}} - T_F - F_I * \omega$$

To calculate this, the motor was simplified to be a block with the thermal mass $m * C_p$, the state of which is determined by the temperature of the block, ΔT. Since the mass of the stator would heat up the fastest, it was used for the mass in the equation and it was assumed to be 60% of the motor's total mass. The stator was also assumed to be made out of iron. The heat flow in, Q_{in}, corresponds to the power dissipation in the motor, and the heat flow out, Q_{out}, is determined by the heat transfer coefficient and the temperature, ΔT. The governing differential equation was found and is shown in equation 2 below. The solution to this equation, assuming the motor starts at ambient temperature, is a first order exponential rising to a final asymptotic temperature.

Equation 2. Governing heat transfer equation for the thermal mass of the motor.

$$\frac{d}{dt}(\Delta T) = \frac{(Q_{in} - \frac{\Delta T}{TPR})}{m * C_p}$$

Using equation 2, an iterative code was run for each motor that plugged in values for Q_{in} until the final ΔT of the motor was just under 75C in 10 minutes. This determined how much power each motor can afford to dissipate in 10 minutes without overheating. Once this new value of $Q_{in,10min}$ was found, it was used in place of the $\frac{\Delta T}{TPR}$ term in the continuous duty equation to obtain the 10-minute duty equation for each motor, shown below in equation 3.

Equation 3. Equation for the safe 10-minute operating torque speed curve of a motor.

$$T_L = \sqrt{\left(Q_{in,10min} - T_F * \omega - F_i * \omega^w\right) * \frac{{K_T}^2}{R_M}} - T_F - F_I * \omega$$

The curves generated from equation 1 and 3 are shown below in figure 17. From these curves, it can be seen that a motor operating for a maximum of 10 minutes at a time can safely operate at higher torques for a given speed compared to a motor operating continuously.

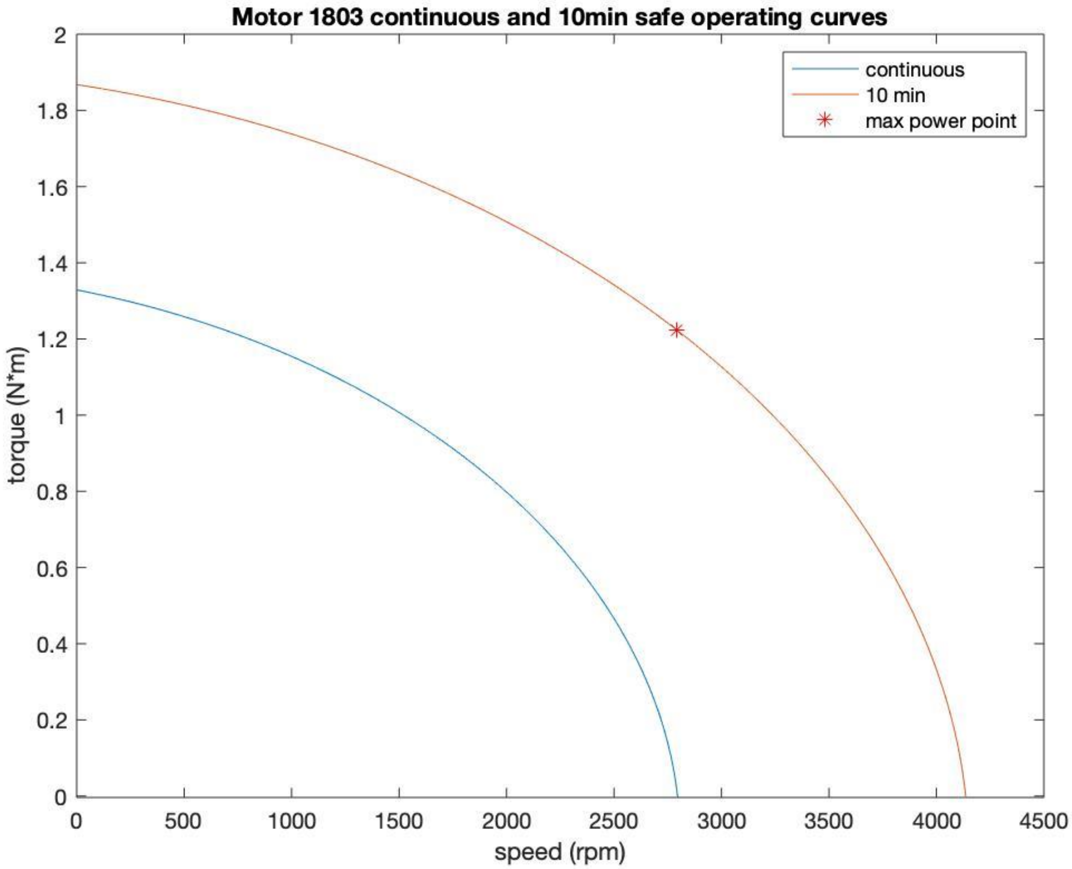

Figure 17. Continuous and 10-minute duty curve for the 1803 motor. The max power point for the 10-minute duty curve is marked with a red star.

From this 10-minute duty curve, the max power point of each motor was found. Using this max power point as the goal, each motor was analyzed to see how many winding changes it would require to operate closest to this max power point. This was done using a code that looked at multiple winding options then selected the winding that allowed the motor to operate closest to this max power point. A representation of this process is shown in figure 18.

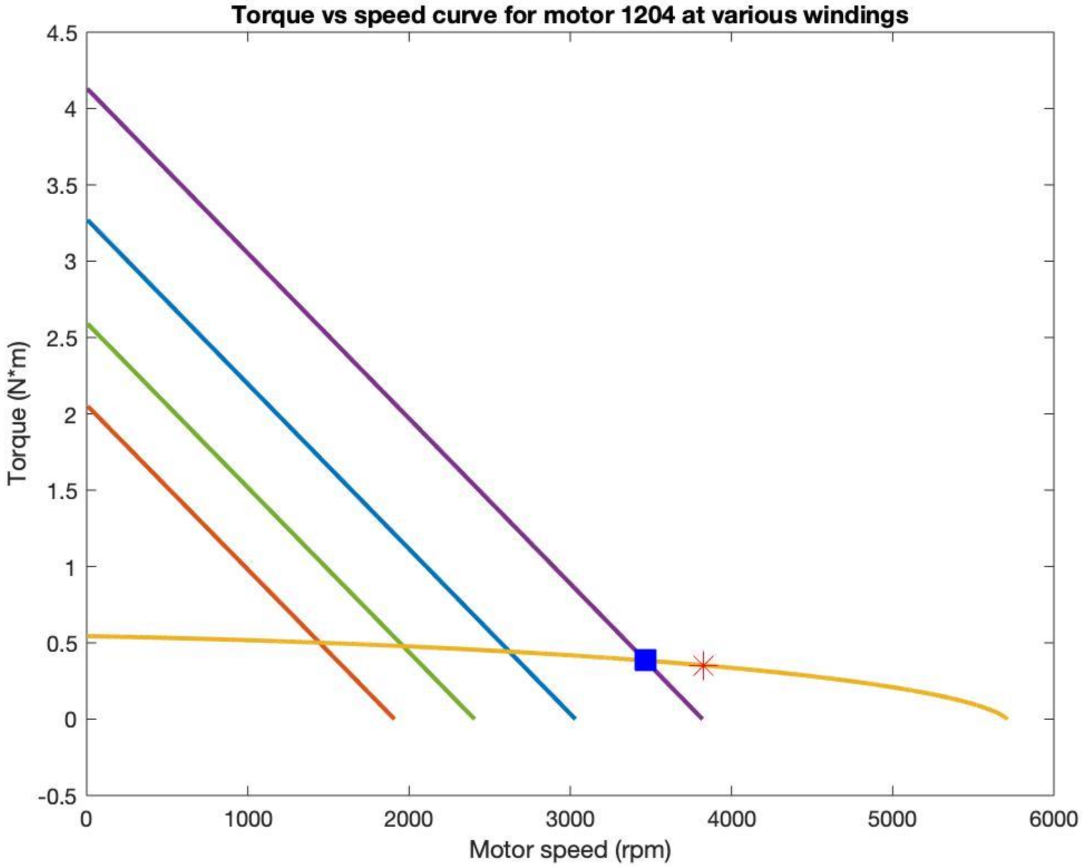

Figure 18. Torque speed curve for the 1204 motor with alternate windings. The orange line represents the nominal windings, with the green, blue, and purple representing 1, 2, and 3 gauge thicker windings respectively. The yellow line represents the safe 10-minute duty curve. The red star represents the max power point on the safe 10-minute duty curve and the blue square represents the max motor power possible with any winding on the 10-minute operating curve.

Once the winding of each motor was decided, the max power each motor could produce while remaining within the 10-minute duty curve was calculated. This max power each motor could produce continuously for 10 minutes was then compared to the power required to open or close the gate in 20 second, shown in appendix 1. After incorporating the efficiency of the gears and lead screw, every motor which could not safely deliver enough power to open the gate in 20 seconds was eliminated. The results from this analysis are shown in appendix 2.

At this point, a gear ratio to accompany each motor needed to be calculated. As shown in figure 16, the torque required to open the gate using the lead screw varies as the gate goes from the open to the closed position. To account for this, a slightly higher than average value for the torque required to rotate the lead screw was calculated and found to be about 1.9355 N*m. Using this value, a gear ratio was found so that each motor could operate at its 10-minute max power torque and speed while delivering the previously calculated average lead screw operating torque via the gear system. This is shown below in equation 4.

Equation 4. The equation used to find the required gear ratio so that each motor can operate at its maximum safe 10-minute power point while delivering the average lead screw operating torque via the gear system.

$$Gear\ Ratio = \frac{average\ lead\ screw\ torque}{\max 10\ minute\ allowable\ motor\ power\ torque}$$

Using this gear ratio calculated in equation 4, a forward integration code was used to validate that each motor could open the gate in the required time without overheating. This forward integration code simulated the operation of each motor, driving the lead screw through the required gear ratio for 20 seconds. At each time point in the code, the motors torque and rpm was calculated as well as the how much the lead screw and gate would move up until the next time point. At each time point, winding, hysteresis, and viscous losses were also taken into account. At the end of the 20 second simulation, the total amount of energy dissipated by the motor was calculated and compared to the total energy required to heat the motor by 75C. From this comparison, I projected how long each motor could run before overheating. This was a conservative calculation as it did account for any heat dissipation from the motor to the environment during the 10 minutes. However, it provides a rough idea for how long the motor might be able to operate. The results from this forward integration code can be seen in appendix 3.

Because the method used to calculate the gear ratio for each motor was based on the lead screws average operating torque, the forward integration results showed that some motors would overheat in less than 10 minutes of operation. While part of this result can be explained by the conservative calculation described above, another reason for this is demonstrated in figure 19. Torques higher than the average lead screw operating torque cause the motor to operate outside of the 10-minute duty curve. This means that the motor could potentially overheat in less than 10 minutes, depending on how long it has to operate at these torque and speed points outside the 10-minute duty curve. While this is cause for some concern, the results in appendix 3 using even the conservative calculation showed that most motors would take 7 minutes or more to overheat, which was taken to be acceptable.

Additionally, in some of the results from the forward integration code, shown in appendix 3, some motors are not able to fully open the gate in 20 seconds even though they are shown to produce more than enough power. This is likely also due to the significant fluctuation in the required lead screw actuation torque. Because of the gear ratio chosen, there are times during the operation of each motor when the motor will produce less than the max power, such as when the torque requirements are below the average lead screw operating torque. When this happens, it drags down the average power the motor is producing over the 20 seconds. In some cases, the average power can reduce enough that the gate is not able to go through the full open and closing cycle.

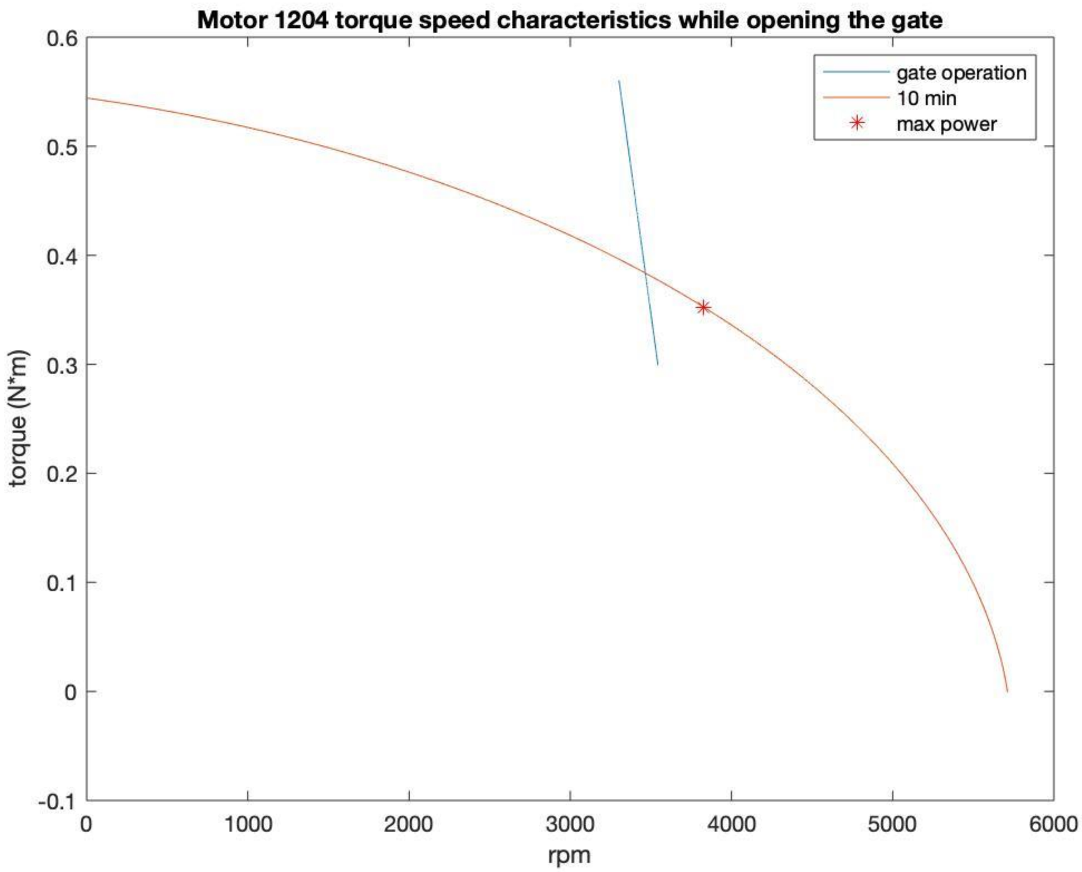

Figure 19. Plot shows the 10 minute safe operating envelope for motor 1204 and the torque and speed operating line the motor undergoes while moving the gate.

In terms of motor selection, one of the most important criteria besides performance was the cost of the motor. Because the motor handout does not list cost, it was assumed that the more mass the motor has the greater it costs.

Given this cost consideration, and the results shown in appendix 3, motor 1204 with 3 gauge thicker windings was selected. This motor was selected because the forward integration code validated it could open the gate in about 17.7 seconds, while taking only 8 minutes and 20 seconds to overheat (which is a conservative calculation as described above). This is also the motor with the smallest mass that was projected to be able to open the gate in time according to the forward integration results. This motor also requires a low gear ratio of 6 to be attached in order to open and close the gate. This low gear ratio requirement is advantageous as it will likely require minimal space and be fairly simple to design.

C) Gear design and selection

From the calculations discussed in the motor selection part of this report, a gear ratio of 6 was required for the selected motor. A plot of gear ratio vs approximate weight for 1, 2, and 3 stage gear sets is shown below in figure 20. From this plot it can be seen that for the required gear ratio of 6, a single stage gear system would weigh the most and a two-stage system would weigh the least. However, as the motor and lead screw require relatively low torques, a subtitle gear system would not need to be very large. Because of this, a one stage gear system was selected for simplicity. Even though a single stage system would weigh the most, it would only weigh 25% more than the lightest of the three stage options which isn't significant given that the gear ratio is small to begin with.

The gear design calculations are shown in appendix 4 along with all the assumptions that were made in the process. The gear and pinion were designed around the max torque and rpm of the motor, 0.56 N*m at 3300 rpm, as here it will experience the greatest stress. The gear and pinion were assumed to be made from hardened steel comparable to options found on Matweb, shown in appendix 6. The gear and pinion had a core and surface hardness of 350 Bhn and a machined surface. The final gear system specifications are listed in appendix 5.

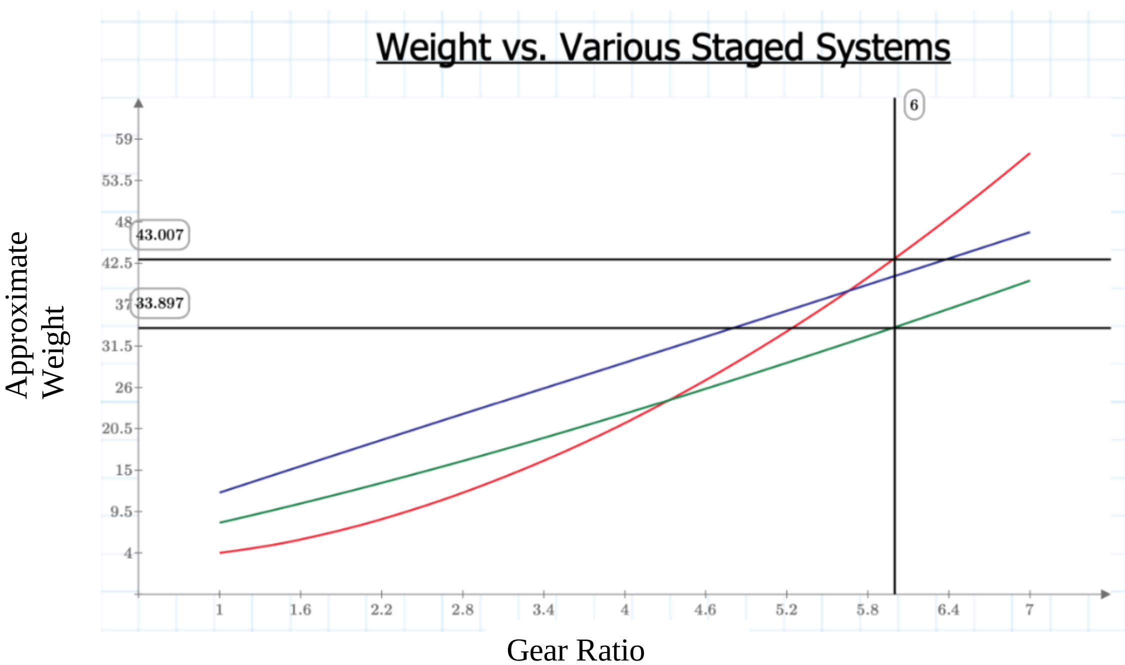

Figure 20. A plot showing gear ratio vs approximate weight. The red line represents a single stage, the green line represents two stages, and the blue line represents three stages.

5. Configuration Layout

The assembly layout for parts of the lead screw system is shown in the drawing at the end of this document. The drawings detail the location of the gears, lead screw, and motor without any mounting components that would be necessary to connect the screw to the gate or protect it from the weather. This drawing is only intended to convey the internal layout of the components within the assembly.

In this assembly layout, the motor, gear system, and bolt are mounted in a fixed location. When the motor turns on, it rotates the gears and the bolt, which force the screw to move either away from the motor or towards it, depending on the direction of the motor's rotation.

The assembly was designed to take up minimal space. Because of this, the motor, gear reducer, and lead screw axes are all oriented parallel to each other. The motor and bolt shown in the drawings are strategically placed so that the screw can extend to its full length and still have a few inches of screw left when the gate is open as a safety measure.

This assembly could be covered in a weatherproof housing so that the all the internal components are protected. Within the weatherproof housing some electronics would also need to be stored, but this is beyond the scope of this project, so they were not detailed.

6. Appendix

1) Power required from the motor to open the gate.

Gate must open in 20 seconds, so the gate must move at 0.75rpm:

$$gate\_rpm = 0.75\ (rpm)$$

Screw efficiency, calculated and discussed in section 4.a. was found to be 38%:

$$\eta_{screw} = 0.38$$

The required gear ratio has not be found yet, but is approximated to be 94%:

$$\eta_{gears} = 0.94$$

The torque required to rotate the gate is 80 lbf*ft:

$$T_{gate} = 80(lbf * ft)$$

Power required from the motor to open or close the gate fully in 20 seconds:

$$motor\_power\_requirment\ = \frac{gate_{rpm} * T_{gate}}{\eta_{screw} * \eta_{gears}} = 23.849\ (W)$$

2) Motor analysis results

This table shows the required winding for each motor to operate closest to the max power point on the 10-minute duty curve developed. The torque, RPM, and max power of each motor at its optimal winding is also listed. The green boxes in the max motor power column detail which motors provide enough power to open the gate in under 20 seconds.

Motor	Winding Change	Torque of Max Motor Power (N*m)	RPM of Max Power	MAX Motor Power (W)
400	0	0.00416248	18600.4378	2.894489373
401	0	0.00976406	12903.0925	4.710001604
402	0	0.011888	11715.9392	5.206942121
500	-1	0.01302689	11779.0368	5.736502687
501	-2	0.0234939	9578.9688	8.413385011
502	-2	0.03811601	7200.71405	10.26076778
700	-2	0.03959153	9494.76922	14.05346893
701	-3	0.07248574	7037.75243	19.07143576
702	-3	0.10410684	6142.48611	23.9067358
703	-3	0.14344643	5234.94892	28.07366019
704	-3	0.19071611	4717.90287	33.63823612
1200	-2	0.07737478	5999.52098	17.35453007
1201	-3	0.16187588	4633.28307	28.03934236
1202	-3	0.22961916	4032.94028	34.61997417
1203	-3	0.29286547	3862.91478	42.29413316
1204	-3	0.38363217	3465.77391	49.70637412
1205	-4	0.43838466	3845.53213	63.024386
1500	-4	0.12154966	5719.75912	25.99132005
1501	-4	0.30049178	3460.207	38.87151899
1502	-4	0.40979832	3077.47791	47.14785638
1503	-4	0.54528809	2876.92979	58.64785131
1504	-4	0.72348425	2491.37841	67.38536931
1505	-5	0.66722346	3060.3001	76.33648457
1506	-5	0.82941919	2900.49539	89.93797225
1800	-4	0.32135974	4152.54937	49.88880605
1801	-5	0.62233944	3329.00415	77.45304442
1802	-5	0.96537801	2859.69573	103.2081664
1803	-5	1.26681334	2690.0457	127.3999091
1804	-5	1.60132252	2445.93121	146.4265684
1805	-5	1.89916632	2314.95798	164.3625781

3) Forward integration results

Motor	Final gate angle (deg)	Time to open (s)	Gear Ratio	Energy dissipated during opening (J)	Minutes of allowed continuous use	Motor mass (kg)
703	49.420	20.000	15.958	297.746	6.961	0.329
704	61.000	20.000	12.002	324.355	7.439	0.383
1200	29.757	20.000	29.584	255.447	4.982	0.202
1201	49.487	20.000	14.141	324.408	7.263	0.374
1202	63.368	20.000	9.969	361.337	7.811	0.448
1203	83.662	20.000	7.816	405.480	8.110	0.522
1204	90.005	17.726	5.967	403.917	8.391	0.607
1205	90.001	14.089	5.222	442.071	8.082	0.805
1500	45.301	20.000	18.832	449.640	7.076	0.505
1501	74.210	20.000	7.618	485.129	8.168	0.629
1502	90.001	18.655	5.586	511.158	8.542	0.743
1503	90.009	15.021	4.198	468.130	8.682	0.859
1504	90.007	13.042	3.164	446.773	9.177	0.998
1505	90.013	11.630	3.431	472.586	8.481	1.094
1506	90.014	9.878	2.760	478.212	8.628	1.326
1800	90.000	17.622	7.123	523.937	8.105	0.765
1801	90.010	11.411	3.678	425.555	8.430	0.998
1802	90.019	8.564	2.371	366.220	8.957	1.216
1803	90.019	6.952	1.807	340.312	9.228	1.434
1804	90.007	6.043	1.429	328.949	9.479	1.638
1805	90.001	5.381	1.205	322.880	9.775	1.862

4) Gear Design and Selection

Gear Stage Calculations

Max torqe produced by the motor: $motor\_T := 0.5602 \cdot N \cdot m$

Max motor torque rpm: $motor\_T\_rpm := 3300 \cdot rpm$

Surface Fatigue Calculations

$$\sigma_H = C_p \cdot \sqrt{\frac{F_t}{b \cdot d_p \cdot I} \cdot k_v \cdot k_o \cdot k_m} \leq S_H = C_{li} \cdot C_R \cdot S_{fe}$$

Assuming the pinion has 18 teeth..
Safety factor of 1.1

$N_p := 18$ $\quad N_g := N_p \cdot 6 = 108$ $\quad b(P) := \frac{14}{P}$

$V(P) := 3.1415 \cdot \left(\frac{18}{P}\right) \cdot 3300 \cdot \frac{1}{12}$ units of ft/min

$kv(P) := \frac{1200 + V(P)}{1200}$ From Fig 15.24 - Assuming hardness less than bhn=350 and shaping cutters are used

$km := 1.6$ From Table 15.2 - Assuming facewidth 0-2 in and less rigid mountings, less accurate gears, contact across the full face

$ko := 1$ From table 15.1 - Assuming uniform power and machinery

$Ft(P) := \frac{0.263 \cdot 33000}{V(P)}$ units of lbf

$I := \frac{\sin(20\ deg) \cdot \cos(20 \cdot deg)}{2} \cdot \frac{6}{7} = 0.138$

$S_{fe}(bhn) := (0.4 \cdot bhn - 10) \cdot 1000$ units of psi

$365 \cdot 8 \cdot 10 \cdot 3300 \cdot rpm \cdot 20 \cdot s = 2.018 \cdot 10^8$ Assuming gears work for 10 years being used 8 times a day for 365 days a year.

$C_{li} := 0.9$ from figure 15.27 assuming 10^8 cycles

$C_R := 1.0$ From table 15.6 assuming 99% reliability

$C_p := 2300$ units of (psi)^0.5. From table 15.4a, for steel gears and pinions

Solving for P....

$P := 20$

$$C_p \cdot \sqrt{\frac{Ft(P) \cdot 1.1}{\left(\frac{14}{P}\right) \cdot \left(\frac{18}{P}\right) \cdot I} \cdot (kv(P)) \cdot ko \cdot km} = S_{fe}(350) \cdot C_R \cdot C_{li}$$

$\text{find}(P) = 41.12$

$P := 40$ Set P to be the standard pitch of 40, recheck values...

$$\sigma_H := C_p \cdot \sqrt{\frac{Ft(P) \cdot 1.1}{\left(\frac{14}{P}\right) \cdot \left(\frac{18}{P}\right) \cdot I} \cdot (kv(P)) \cdot ko \cdot km} = 1.126 \cdot 10^5$$

$$S_H := S_{fe}(350) \cdot C_R \cdot C_{li} = 1.17 \cdot 10^5$$

$\sigma_H \le S_H$ is valid with P=40/in

Checking the contact ratio....

$$r_p := \frac{\left(\frac{N_p}{2}\right)}{P} = 0.225 \qquad r_g := \frac{\left(\frac{N_g}{2}\right)}{P} = 1.35 \qquad a := \frac{1}{P} = 0.025 \qquad c := r_p + r_g = 1.575$$

$$r_{ap} := \frac{\left(\frac{N_p}{2}\right)}{P} + a = 0.25 \qquad r_{ag} := \frac{\left(\frac{N_g}{2}\right)}{P} + a = 1.375 \qquad r_{bg} := (r_g) \cdot \cos(20 \cdot deg) = 1.269$$

$$r_{bp} := (r_p) \cdot \cos(20 \cdot deg) = 0.211$$

$$p_b := \pi \cdot \frac{18}{P} \cdot \frac{\cos(20 \cdot deg)}{18} = 0.074$$

$$CR := \frac{\sqrt{r_{ap}^2 - r_{bp}^2} + \sqrt{r_{ag}^2 - r_{bg}^2} - c \cdot \sin(20 \cdot deg)}{p_b} = 1.695$$

Valid contact ratio. From this we can assume there is partial sharing of the surface fatigue load in the following fatigue calculations.

Bending Fatigue Calculations

$C_L := 1$

$C_G := 1$ since P>5

$C_S := 0.69$ From fig 8.13 - Assuming a hardness of 350 bhn and a machined surface finish

$kr := 0.897$ From table 15.3 - Assuming 90% reliable

$kt := 1$ Assuming temp < 160F

$kms := 1.4$ for input and output gears

$Ft := 0.56 \cdot P = 22.4$ units of lbf

$b := \frac{14}{P} = 0.35$ units of in

$J := 0.27$ From fig 15.23.a - Assuming partial sharing

$kv := kv(P) = 1.324$

$ko := 1$ From table 15.1 - Assuming uniform power and machinery

$km := 1.6$ From Table 15.2 - Assuming facewidth 0-2 in and less rigid mountings, less accurate gears, contact across the full face

Solving for Sn'...

Guess Values

$Sn' := 30000$

Constraints

$$Sn' \cdot C_L \cdot C_G \cdot C_S \cdot kr \cdot kt \cdot kms = \frac{Ft \cdot P}{b \cdot J} \cdot kv \cdot ko \cdot km$$

Solver

$\mathbf{find}(\mathbf{Sn'}) = 2.318 \cdot 10^4$

These results show the gears need a core strength of over 23,180 psi, easily acheived with steel

5) Final Gear Specifications

$Total\_GR := 6$

$P := 40 \cdot \frac{1}{in}$ $\quad b := \frac{14}{P} = 0.35\ in$ $\quad \phi := 20 \cdot deg$

$N_p = 18$ $\quad N_g = 108$

$d_p := \frac{N_p}{P} = 0.45\ in$ $\quad d_g := \frac{N_g}{P} = 2.7\ in$

$CR = 1.695$

6) Possible steel used for the gear design

http://matweb.com/search/datasheet.aspx?MatGUID=a3cb537b777b4fe299c658b23d43378b

Physical Properties	Metric	English
Density	7.85 g/cc	0.284 lb/in³

Mechanical Properties	Metric	English
Hardness, Brinell	385	385
Hardness, Knoop	415	415
Hardness, Rockwell B	101	101
Hardness, Rockwell C	42	42
Hardness, Vickers	408	408
Tensile Strength, Ultimate	1380 MPa	200000 psi
Tensile Strength, Yield	1170 MPa	170000 psi
Elongation at Break	15 %	15 %
Reduction of Area	48 %	48 %
Modulus of Elasticity	205 GPa	29700 ksi
Bulk Modulus	160 GPa	23200 ksi
Poissons Ratio	0.29	0.29
Machinability	65 %	65 %
Shear Modulus	80.0 GPa	11600 ksi
Izod Impact	22.0 J	16.2 ft-lb